Journal of Environmental Management 251 (2019) 109610

Contents lists available at ScienceDirect

Journal of Environmental Management

journal homepage: www.elsevier.com/locate/jenvman

Research article

Effects of magnesium ferrite biochar on the cadmium passivation in acidic soil and bioavailability for packoi (*Brassica chinensis* L.)

Xing Gao[a], Yutao Peng[a,c], Yaoyu Zhou[b,c], Muhammad Adeel[a], Qing Chen[a,*]

[a] Beijing Key Laboratory of Farmland Soil Pollution Prevention and Remediation, College of Resources and Environmental Sciences, China Agricultural University, Beijing, 100193, China

[b] College of Resources and Environment, Hunan Agricultural University, Changsha, 410128, China

[c] Department of Civil and Environmental Engineering, The Hong Kong Polytechnic University, Hung Hom, Kowloon, Hong Kong, China

ARTICLE INFO

Keywords:
Modified biochar
Magnesium ferrite
Cadmium
Adsorption
Soil remediation

ABSTRACT

Biochar (BC) and magnesium ferrite (MF) have been used in effective adsorption of cadmium (Cd) in aqueous environment, whereas little is known about the effect of their composite on Cd adsorption and Cd-contaminated soil remediation. In this study, biochar (BC), magnesium ferrite (MF) and biochar assembled with magnesium ferrite (MB) were prepared for Cd adsorption and then applied in soils (1–2% *w/w*) to investigate their effects on Cd passivation by performing leaching experiments and early stage seeding growth test for packoi (*Brassica chinensis* L.). Compared with the BC and MF, the MB showed greater adsorption property for Cd at aqueous solution (31.3 mg/g) and amended soils (1.85 mg/g at 2% applied rate) based on the isotherms studies. Besides, the MB performed the better passivation ability in reduction of the bioavailable Cd and seeding growth experiment. Solid state analysis of the materials before and after leaching indicated that the passivation mechanism may be dominated by ion exchange and surface complexation. Principal component analysis revealed that the soil pH and adsorption capacity had the strong correlation with the contents of bioavailable-Cd and seedling growth. These results indicated that MB could be used as an efficient amendment in Cd contaminated soil for reducing bioavailable Cd concentrations and improving plant growth.

1. Introduction

Heavy metal (loid)s contamination in Chinese agricultural land has received significant attention in recent years (Liu et al., 2019a; Yin et al., 2019). For example, it has been reported that the mean concentration of cadmium (Cd), most toxic environmental pollutants, in many southern provinces (*e.g.* Guangdong provinces (n = 1424) was higher than the environmental quality standards (GB 15618-2018) (Chen et al., 2015), and therefore it attracted more attentions owing to accelerated pace of industrialization and increasing demand for chemicals (Bashir et al., 2019; Liu et al., 2019b; Liu et al., 2019c). Accordingly, excessive Cd accumulation in soils caused adverse impact on crop yield and quality, ultimately to the human beings through food chain. There are various well-developed strategies to remediate the Cd-polluted agricultural soils, *e.g.* phytoremediation, chemical immobilization, microbial remediation (Garrido-Rodriguez et al., 2014; Gong et al., 2018; Liu et al., 2019d; Xia et al., 2017). Among them, in situ remediation techniques is a promising and cost-effective method in this field due to its simple operation, little/no disruption to soils, wild applicability and high efficiency. The mechanisms of the Cd passivation in soil includes adsorption, binding and precipitation, which result in the interruption of Cd transferring in soil-plant system.

Various amendments have been proposed for Cd-contaminated soil remediation, such as lime (Pardo et al., 2018), clay mineral (Xu et al., 2017), compost (Rehman et al., 2018) and biochar (Cui et al., 2019b; Li et al., 2019). Biochars, the porous carbonaceous materials produced from myriad of biomass after pyrolysis or gasification progress under low/no oxygen condition (Beiyuan et al., 2017; Fang et al., 2016; Yoo et al., 2018), have attracted considerable attention in soil amelioration because of its distinctive and versatile characteristics including low-cost, carbon sequestration, soil fertility/properties improvement and immobilization/adsorption of pollutants. Recently, Cui et al. (2019b) reported the wheat straw biochar reduced the Cd bioavailability up to ~90% as compared to control (2.5 mg Cd/kg) and exhibited stable property based on the long-term incubation. Puga et al. (2016) reported the sugarcane straw derived biochar effectively reduced the Cd, Pb and Zn in the pore water under acidified soil and thus decreased their mobility, and suggested that the metal adsorption on biochar was the

* Corresponding author.
E-mail address: qchen@cau.edu.cn (Q. Chen).

https://doi.org/10.1016/j.jenvman.2019.109610
Received 6 July 2019; Received in revised form 5 September 2019; Accepted 18 September 2019

primary mechanism. Moreover, the passivation efficiency of pristine biochars could be enhanced through modification techniques through impregnation with metals/metal oxide, etc (Wang et al., 2018a; Xiang et al., 2019a). In order to improve the immobilization efficiency, various modification approaches have been proposed. For example, Wang et al. (2019) showed the concentration of bioavailable Cd decreased after addition of Mn–Fe-coated biochar by 76%, compared with pristine biochar of 47.7%. Wu et al. (2019) indicated sulfur-iron modified biochar could convert more bioavailable Cd to active stable complexes in comparison with untreated biochar, resulted in significant reduction of exchangeable-Cd fraction and higher bacterial abundances. Qiao et al. (2018) reported the addition of zero valent iron (ZVI) and biochar composites reduced bioavailable Cd in soil as well as rice tissue compared to original biochar because of the synergistic effects of biochar and ZVI.

Ferrites, with general formula $MeFe_2O_4$ (Me = Fe, Mg, Mn, etc.), are generally served as an alternative material for water purification because of its easy separation, large adsorption capacity, high stability and cost-efficiency (Gwenzi et al., 2017). It was also reported that manganese ferrite immobilized Cr(V) (Eyvazi et al., 2019) and Cu, As, Pb, Zn (Li et al., 2016) in the soil through the column leaching and batch test, indicating its passivation potential towards heavy metal polluted soil. Nevertheless, pure ferrites are frequently supported by porous carbonaceous materials (*e.g.* activated carbon, biochar, mesoporous carbon, etc.) to avoid the negative layers stacking effect. Thereafter, the enhanced adsorption capacity of the ferrite modified biochar were considerably recorded (Karunanayake et al., 2018; Lu et al., 2018). So far, biochars and ferrites have been used for heavy metal passivation in soil (Eyvazi et al., 2019; Lu et al., 2018; Qiao et al., 2018), but the comparison study of immobilization effectiveness and mechanism among ferrite modified biochar, biochar and ferrite in soil condition has not been reported yet. Compared with other conventional ferrites, the magnesium ferrite showed a better affinity for Cd in our previous experiments and posed no secondary pollution for environment system (Jung et al., 2017). Hence, we the select the magnesium ferrite to modify the pristine biochar and hypothesized that magnesium ferrite modified biochar could perform better in reducing bioavailable Cd and alleviating the Cd-stress on plant growth.

In this study, biochar (BC, produced from corn stalk), magnesium ferrite (MF) and magnesium ferrite biochar (MB) were synthesized and served as the soil amendments to evaluate their performance in Cd remediation. In this study, the efficiency of the three materials was compared by combining the batch experiments, solid-state analysis and early stage growth seedling growth test. Our specific objectives are as follows: (1) to investigate the effect of amendments on Cd passivation efficiency and adsorption capacity at different application rates, (2) to explore the immobilization mechanism in soil through microscopic characterization and (3) to evaluate the effect of amendments on seeding growth for packoi (*Brassica chinensis* L.) in natural Cd-contaminated soil.

2. Materials and methods

2.1. Preparation and characterization of three amendments

In this study, corn (*Zea mays* L.*)* stalk collected in Shangzhuang Experimental Station, Beijing, was employed as biomass to produce biochars. Before use, corn stalk was cleaned with deionized distilled (DI) water several times and subsequently oven-dried at 60 °C overnight, then crushed and sieved through 0.45 mm pore size. All the chemical reagents used to synthesize the materials were of analytical grade and purchased from Sinopharm Chemical Reagent Co., Ltd.

BC was prepared by slow pyrolysis of corn stalk biomass in muffle furnace (Tianjin Zhonghuan Experiment Electric Furnace Co., Ltd.) at 550 °C with 10 °C/min heating rate and 2 h retention time under limited oxygen condition. After cooling to ambient temperature naturally, the BCs were rinsed with DI water several times to remove impurities and then oven-dried at 60 °C for future use.

MB was prepared by post-treatment method according to the modified method reported by Jung et al. (2017). Specifically, biochar slurry was prepared by mixing 10.0 g BC and 400 mL DI water, ultrasonically reacting (SYU-10-200D TD, 40 KHZ, Zhengzhou Shengyuan Instrument.) at 25 °C for 30 min. 0.1 L mixed solution containing 0.022 mol/L $FeCl_3{\cdot}6H_2O$ and 0.011 mol/L $MgCl_2{\cdot}6H_2O$ (total metal: biochar = 1.5 : 10, *wt*%) was added into the BCs slurry and then stirred at 30 °C for 6 h to achieve the fully dispersed suspension. During the stirring process, 5 mol/L NaOH was added drop-wise (~3 mL/min) to adjust the suspension pH to 10.0. The precipitate was obtained by vacuum filtration and then continuously rinsed with DI water and ethanol until the filtrate pH reached 7.0. After that, the resulting composites were oven-dried at 60 °C overnight and then transferred into muffle furnace immediately, kept at 350 °C for 2 h. Finally, the acquired composites were repeatedly cleaned with DI water and oven-dried at 40 °C for 12 h. Before use, all samples were gently crushed and sieved into 0.149 mm. MF was also synthesized according to the same procedure.

Techniques used for characterizing the materials (BC, MF and MB) included scanning electron microscopy-energy dispersive X-ray spectroscopy (SEM-EDX), X-ray diffraction (XRD), Fourier transform infrared spectroscopy (FTIR), and X-ray photoelectron spectroscopy (XPS) analysis. Detailed information for the instruments is given in the Supplementary Information (SI).

2.2. Soil characterization

The soil samples were collected from the surface layer of uncontaminated arable land in Wushan, Guangzhou, China. The chemical properties of lateritic red soil (sandy soil) were given as follow: pH of 5.62, organic matter contents of 18.21 g/kg, and total nitrogen, phosphorus, potassium, magnesium, calcium, iron and aluminum were 0.27, 0.37, 3.80, 0.03, 0.06, 32.26 and 153.4 g/kg respectively.

The air-dried soil was ground and sieved to a particle size inferior to 2 mm, then spiked with cadmium (as $CdCl_2$, analytical grade, Sinopharm Chemical Reagent Co., Ltd) solution to achieve Cd concentration of 2.0 mg/kg dry soil. The spiked soil was supplemented with DI water until reached the 70% water holding capacity (WHC), and mixed uniformly. After that, the soils were stored in the incubation chamber for 21 days at 25 °C with relative humidity of 70%. The Cd concentration in soil was selected referenced from the National environmental quality standards (GB 15618-2018).

2.3. Sorption experiments in aqueous solution

In batch experiments, 0.05 g of three amendments (BC, MF and MB) were mixed with 20.0 mL Cd (II) solution (pH = 6.0) at the concentrations ranging from 5 mg/L to 500 mg/L into the 50 mL glass. The vials were shaken at 180 rpm and 25 °C for 24 h in a thermostat shaker. Suspension was obtained and then filtered through 0.45 μm syringe filters. The Cd concentrations were measured by the atomic absorption spectrometry (AAS; Agilent 204 DUO, USA). The amount of adsorbed Cd at equilibrium, q_e (mg/g) was calculated by the following equation:

$$q_e = \frac{(C_0 - C_e)V}{m} \quad (1)$$

where C_0 and C_e is the cadmium concentration (mg/L) at initial and equilibrium; V (L) and m (g) refer to the solution volume and the adsorbents dosage.

In this studies, Langmuir and Freundlich isotherm equations were chosen to model the data (Xiang et al., 2019b). Two isotherm models are expressed as follows:

$$q_e = \frac{Qe_{max}}{1 + bC_e} \quad (2)$$

$$q_e = K_f C_e^{1/n} \quad (3)$$

where q_e is the amount of adsorbed cadmium at equilibrium (mg/g); C_e is the cadmium concentration at equilibrium (mg/L); Q_{max} is the cadmium adsorption uptake at the maximum level (mg/g); b (L/mg), K_f ((mg/g) $(L/mg)^{1/n}$) and $1/n$ are Langmuir, Freundlich constants and adsorption intensity, respectively.

2.4. Incubation experiments

The effectiveness of BC, MF and MB on Cd passivation in Cd-spiked soil (section 2.2) and Cd leaching were examined by leaching experiments described by Hudcova et al. (2019). Before the incubation, three holes (diameter: 10 mm) were created at the bottom of plastic pots and then covered by nylon net filters (size: 0.074 mm) and silica sand to retain the soil during leaching experiment. BC, MF and MB were transferred into plastic pots with the rate of 1% and 2%, respectively. Two types of experiments (A, B) were conducted as shown in Fig. S1. Specifically, for the experiment A, the Cd-spiked soil mixed with materials (total weight of soil and material mixture was fixed at 100 g) homogenously and then placed above the nylon net filters. As for experiment B, the materials were placed above the silica sand layer and covered by the double-layered nylon net filters and then Cd-spiked soil. Besides, a control variant (without passivation agents) for treatment A and B were also provided. After covered with plastic films from the top, all pots were randomly placed into the incubation chamber at 25 °C with relative humidity of 70% for 30 days.

Leaching experiments were conducted with 3 days interval by adding 30 mL DI water uniformly each time from top of the pot and collected the leachate after 12 h (preliminary experiments showed that the volume of leachate remained the same after 8 h). The leachate of each treatment was collected and filtered with 0.45 μm syringe filter. And the pH, EC and Cd concentrations were measured subsequently. After the 30 days incubation, the air-dried soils of treatment A were ground and sieved to a particle size inferior of 2 mm for measuring the pH, EC and the bioavailable Cd by 0.01 M $CaCl_2$ extraction method (Houba et al., 2008; Lu et al., 2017). The extraction procedure was conducted in triplicates. Materials from the treatment B (2% *w/w*) were collected from the double layered nylon net filters for further characterization (same as the part 2.1.) to explore the immobilization mechanism.

2.5. Soil adsorption study

Soil adsorption experiments were performed using the method described by Khan et al. (2018) with some modifications. Briefly, after 30 days incubation and treatment described in "section 2.4", 0.8 g of air-dried soil samples from experiment A was transferred into the 50 mL glass vial containing 20 mL Cd (II) solution (pH = 6.0), with concentration ranging from 5 to 500 mg/L. To better understand the change of the sorption affinity towards Cd, higher concentration (i.e. 500 mg/L) was selected according to the relevant work (Khan et al., 2018; Loganathan et al., 2012; Shi et al., 2007). The rest of the experiment procedures and data analysis was the same as "section 2.3".

2.6. Early stage seeding growth bioassay

To further confirm the impact of BC, MF and MB on Cd phytotoxicity as well as plant growth, early-stage seeding growth bioassay experiment for packoi (*Brassica chinensis* L.) were conducted in natural Cd-polluted soil. After 30 days stabilization of amended natural soil, 30 packoi seeds were sown on the 30 g natural contaminated soil (sampled from surface layer of paddy soil at Liaoyuan village, Zhuzhou, Hunan, China, pH of 4.5, total cadmium: 2.66 mg/kg) mixed with amendments (application ratio was same with section 2.4) in the Petri dish (diameter: 90 mm) in triplicate. During the experiments, the petri dishes were placed in a thermostatic chamber with temperature of 25 °C and daily weighted to maintain 70% WHC by supplementing DI water. After 3 days of incubation, the seed germination rates were counted and each germinated seed was collected to determine the total root/shoot length using a caliper ruler. Significant protrusion was recognized as the criterion for germination (Wang et al., 2018b).

2.7. Statistical analysis

The statistical analysis was performed using SPSS 20.0 (SPSS Inc., USA). The significant differences in the leachate of pH, EC, Cd concentration and soil properties, bioavailable Cd and roots/shoots length among different treatments were evaluated using Duncan's multiple range tests and One-way analysis of variance (ANOVA) ($P < 0.05$). Principle component analysis (PCA) was carried out to identify the soil and seeding characteristics among the treatments using the Canoco 5.0.

3. Results and discussion

3.1. Characterization of newly synthesized materials

The XRD patterns (Fig. 1a) of synthesized MF and MB are similar with the common XRD pattern of the pure magnesium ferrite. The corresponding diffraction peaks can be indexed by a JCPDS X-ray powder diffraction file of No. 73–2211, which indicated that the BC was successfully modified by MF and provided more active adsorption sites for contaminants. Besides, the silicon dioxide (JCPDS X-ray powder diffraction file of No. 78–1253) existed at the surface of the BC and MB which can be ascribed to the strong absorption capacity of gramineae plants to Si and the silica inside the biomass was transformed to silicon oxide after pyrolysis (Yang et al., 2018).

The SEM images (Fig. 2) displayed the morphological properties of the materials. As for the magnesium ferrite (Fig. 2c), the corresponding image revealed that the each grain is spherical and very small, leading easily to form agglomeration (Mahato et al., 2017). As shown in Fig. 2a and b, biochar with and without modification presented distinctive porous structure and small canals because of the release of the volatile matter during the pyrolysis process. Compared to the BC, the MB surface appeared to be coarser after the introduction of the MF, implying the successful loading of the irregular MF particles on the biochar surface. Additionally, the SEM/EDX analysis of MB consisted of the higher contents of the alkaline metal (especially for Mg) and Fe than that of BC, confirmed by the corresponding peaks observed in the MB, which also supported the incorporation of magnesium ferrite particles.

The FTIR spectra of the materials were presented in Fig. 1b. For the ferrite materials (*i.e.* MF and MB), the broad absorption bands ranged from 520 cm^{-1} to 800 cm^{-1} was associated with the metal-oxygen bonds (Fe/Mg–O and O–Fe/Mg–O) (Mahato et al., 2017; Yang et al., 2019), which is absent in the untreated biochar, suggesting the impregnation of MF on the biochar matrix. As for the biochar samples, the absorption band around 1600 cm^{-1} and 2900 cm^{-1} could be assigned to the C=C and C–H stretching vibration, respectively (Yin et al., 2018). The band around 1020 cm^{-1} was ascribed to the C–O stretches, indicated the presence of various functional groups including ester, hydroxyl, and carboxylate moieties (Yang et al., 2018; Yin et al., 2018). Thus, the synthesized magnesium ferrite biochar possesses abundant and diverse surface oxygen-containing functional groups, metal-oxygen bonds as well as amorphous ferrite structure, which may provide extra adsorption sites and promote the formation of Cd-ligand complexes, thus leading the higher adsorption (Trakal et al., 2016).

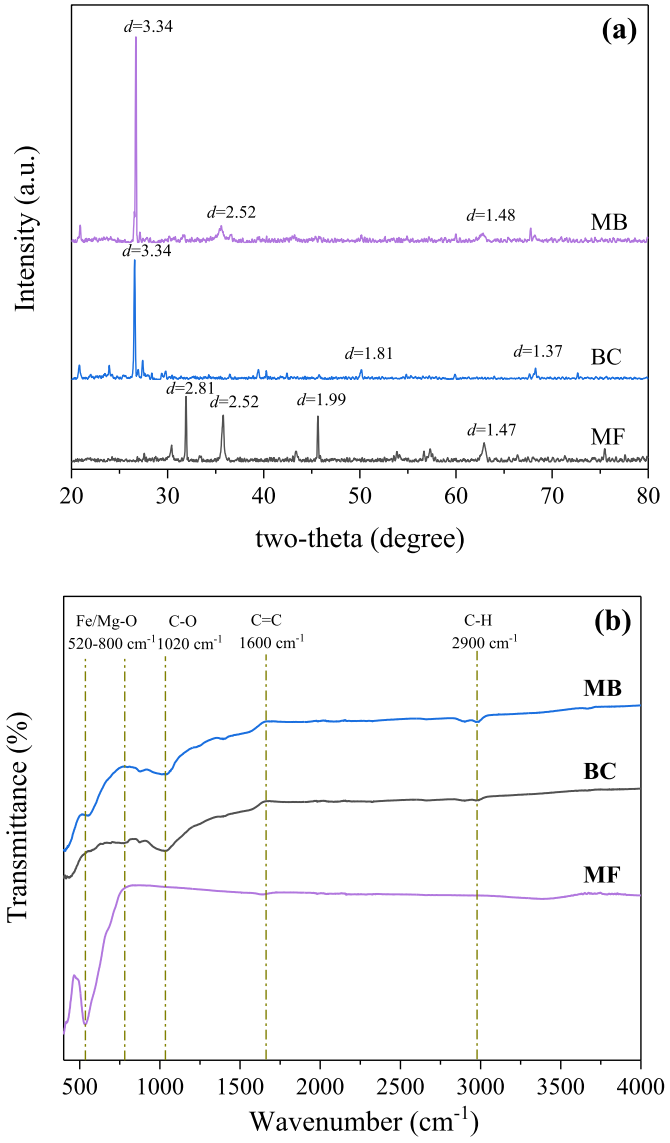

Fig. 1. XRD (a) and FTIR (b) spectra of MB, BC and MF.

3.2. Cadmium adsorption isotherm in aqueous condition

The cadmium sorption isotherms fitted with Langmuir and Freundlich onto three materials were shown in Fig. 3a, while the corresponding parameters data was plotted in Table S1. Langmuir model better fitted with isotherm data for all materials indicated that the cadmium sorption process took place on monolayer and single-molecule of those materials. According to the Langmuir fitting, the maximum cadmium adsorption capacity of BC, MF and MB reached 20.86, 17.33 and 31.27 mg/g, respectively. Compared to the BC and MF, the MB exhibited relatively higher ability to adsorb Cd.

The phenomenon that ferrite biochar has a higher adsorption capability towards heavy metals than pure ferrite could be due to the following reasons. The BC and MB have the same biochar functional group. The enhanced adsorption ability might be attributed to the extra/secondary positive sites of metal-oxygen bond and additional portion of its surface area induced by the precipitated MF (Karunanayake et al., 2018). Similarly, Peng et al. (2019b) highlighted the importance of the prevention of stacking effecting by biochar carrier, which promoted the well-dispersion of the MF, leading greater adsorption performance for heavy metal.

3.3. The pH and Cd concentration in the leachate

The pH increased most significantly by applying MB, which was obtained at both application rates (1% and 2%) (Fig. 4). The elevated leachate pH by biochar and metal oxides in the acidic soil was largely reported (Beesley and Marmiroli, 2011; Hudcova et al., 2019; Yin et al., 2016) which is probably caused by the dissolution of the alkaline components (*e.g.* primary functional groups and ash contents on the biochar) and H^+ consumption/replacement for the MF (Liu et al., 2018; Puga et al., 2016). The pH of leachate in 1% and 2% MB increased most significantly may be ascribed to the following reasons. First, the acid-catalyzed effect caused by the oxidation of the iron-based materials accelerated the neutralizing process (Peng et al., 2019a), which may play a crucial role in acidity alleviation. Second, the formation of a complex between iron-based particles and biochar with metal ions may facilitate the reduction of H^+ in the leachate (Cui et al., 2019a). Generally, the MB exhibited the very similar alkaline pH with BC while the ferrite showed the circumneutral characteristics, thus the chemical properties combined with strong complexation effects ultimately attributed to the highest increase of the leachate pH.

However, Cd was not detected in leachate among all treatments. This phenomenon may be due to relatively low Cd contents in soil (2 mg/kg) as compared to (Puga et al., 2016) and (Qin et al., 2018) of which the Cd contents in the tested soil were higher than 10 mg/kg and extremely low Cd concentration in the leachate was obtained.

3.4. Effect of the amendments on cadmium bioavailability

In general, three materials significantly ($P < 0.05$) reduced the $CaCl_2$-extractable Cd concentration and exhibited greater performance at 2% application rate (Fig. 5). Furthermore, MB was more effective in reducing the bioavailable-Cd than BC and MF, which decreased the bioavailable-Cd by 98.0% at 2% application rate. This result indicated that the incorporation of three materials facilitated Cd retention in soil. Previous studies also proved the Cd passivation effectiveness of the biochar (Qin et al., 2018), ferrite (Li et al., 2016) and ferrite biochar (Lu et al., 2018), which could be explained by the material-induced soil pH increase as well as soil adsorption capacity for Cd (Qin et al., 2018). In this study, a significant correlation between soil pH and Cd concentrations was observed (see PCA results in **3.8**), indicating the soil pH was a critical factor in cadmium passivation. The result was consistent with the Lu et al. (2017), who demonstrated that the significantly negative correlation between soil pH and $CaCl_2$-extractable Cd. Generally, the increased soil pH promoted the precipitation of Cd hydroxides and carbonates phases and led to deprotonation of the soil surface, which could generate more negative surface charge and increase the affinity towards the Cd (Yin et al., 2016). Apart from the pH, the elevated adsorption ability of amended soils could be considered as another factor of the bioavailable Cd reduction, which will be further discussed in section 3.5.

3.5. Effect of the amendments on cadmium adsorption of soil

The cadmium adsorption isotherms of soil with and without amendments were shown in (Fig. 3b and c), while the fitted data were presented in (Table 1). The related parameters of isotherm models indicated that the Cd adsorption process of soil was well fitted by Langmuir model with higher R^2 value and the sorption capacity increased after the addition of amendments (Table 1), suggesting the monolayer and homogenous adsorption sites existed on the surface of the red soil and it provided additional adsorption sites for Cd. Similarly, the constants of two models (*b* and *n* for Langmuir and Freundlich, respectively) were much greater for amended-soils as compared to control, indicating the higher sorption capacity and stronger affinity towards Cd. With the introduction of 2% MB, it exhibited the greatest improvement for Cd sorption affinity and significantly increased the Cd

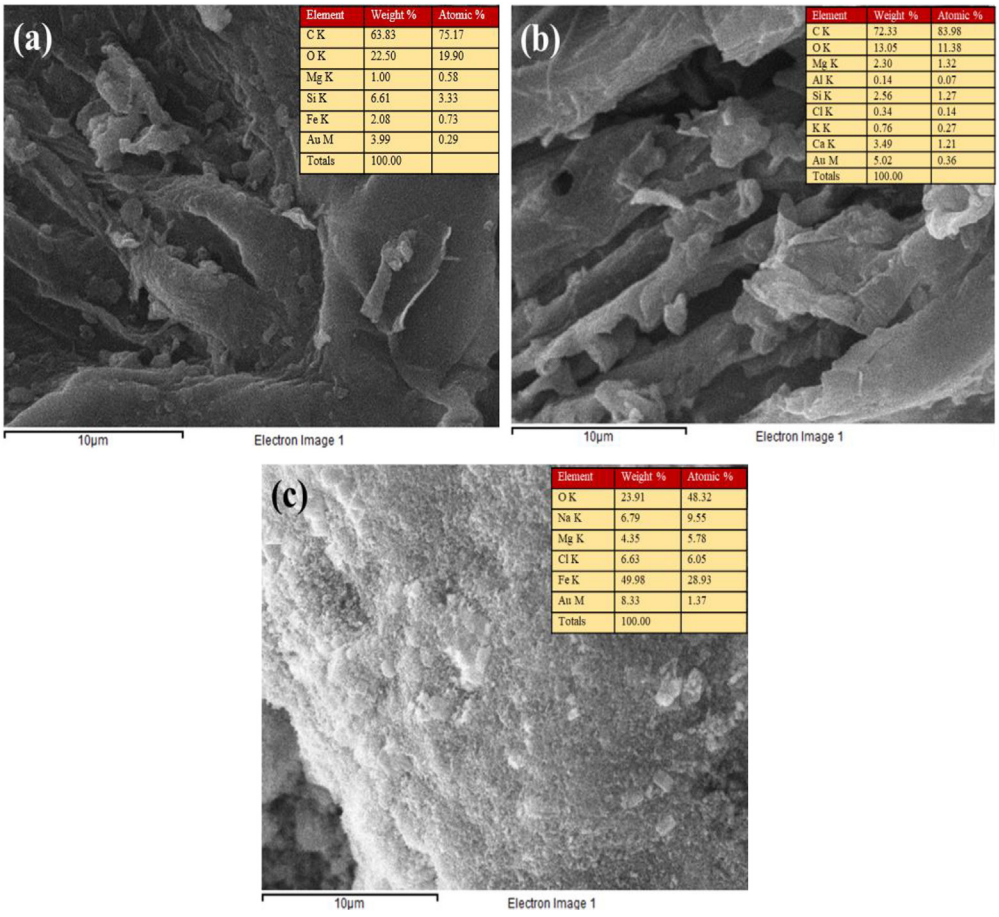

Fig. 2. SEM and EDS images of MB (a), BC (b) and MF (c).

adsorption capacity, adsorption constants (*b* and *n*) by 2.1, 3.6 and 1.38 folds as compared to control, respectively. It demonstrated that the low-affinity sorption sites elevated after the incubation with the amendments, which in turn promoted the adsorption of the Cd ions through specific adsorption process (*e.g.* chelated with Cd (Khan et al., 2018)) and effectively reduced the bioavailable-Cd. The enhanced adsorption affinity of MB-amended soil to Cd could be attributed to the evaluated soil pH and organic matter since the tested soil had a lower pH Table 2 and extra adsorption sites provided by the functional groups (*e.g.* hydroxyl, carboxyl and metal-oxygen bond) which is in favor of the formation of the stable Cd-complexes/precipitates (Wu et al., 2019).

3.6. Passivation mechanism

The surface characterizations of BC/MF/MB after leaching experiments were also performed to better understand the Cd passivation mechanism. The strong impurity peaks in XRD patterns of silicon dioxide and sodium chloride weaken or disappeared among all treatments (Fig. S2). It may be attributed to the dissociation and ion exchange (such as Na^{+}, Ca^{2+} and Mg^{2+}) between soil-amendments matrix and Cd^{2+} (Igalavithana et al., 2017) which corresponded to the EC analysis (Table S2). However, no strong peak in regarding to cadmium compound was found on the surface of these samples due to the low Cd content in leachate.

The strong absorption band from 520 cm^{-1} to 800 cm^{-1} in FTIR spectra (Fig. S3), corresponding to metal-oxygen bond (Yang et al., 2019), significantly strengthen after the leaching experiment, suggesting the Cd^{2+} could be absorbed via metal-oxygen bond (Ouředníček et al., 2019). The shifts at 2900 cm^{-1} and 1020 cm^{-1}, belonged to binding vibration of C–O and C–H, respectively, indicated that the functional groups on the biochar, such as hydroxyl, carboxylate and phonic hydroxyl, also played an essential role during passivation process via Cd-ligands coordination bonds.

The XPS surveys of BC, MF, and MB before and after leaching experiments were showed in Figs. S4 and S5. The C1s peaks at binding energies of 286.1, 288.9 and 288.0 eV corresponding to C–O, O═C–O and C═O in the BC and MB were shifted to 288.2, and 286.7 eV, respectively. Furthermore, the O1s peaks at binding energies of 532.5 and 532.0 eV corresponding to O═C were reduced by 0.2–0.5 eV, meaning the hydroxyl and carboxylic groups may take part in the Cd passivation process (Chen et al., 2018; Wan et al., 2019). Fig. S5a'''–d''' showed that the peak intensity of 711.2 eV (2p 3/2), 724.8 eV (2p 1/2) of Fe2p (Mittal et al., 2004; Xiong et al., 2019) decreased by 0.2–0.5 eV, which could be ascribed to the Cd^{2+} bound on the surface of the Fe-oxides or the formation of Fe–O–Cd complexes (Trakal et al., 2016). In the Mg1s spectra, a typical $MgFe_2O_4$ peak of Mittal et al., 2004 was shifted to 1303.6 eV (corresponding to Mg–O), suggesting the Cd passivation occurred through aging process and interaction between the Mg^{2+} and Cd^{2+} (Igalavithana et al., 2017).

Based on the analysis above, the mechanism of the Cd passivation of BC/MF/MB may mainly consist of the outer-sphere surface complex and ionic exchange. The Cd could be coordinated with oxygen-containing functional groups and Mg/Fe oxides composites on MB to form stable chelate complex (*e.g.* O═C–O–Cd, -C-O-Cd, $(Mg/Fe\text{-}R\text{-}O)_2$-Cd (Lin et al., 2018)). The cation (*e.g.* Ca^{2+}, Mg^{2+}), induced by the decomposition of the amendments, may be also involved in the adsorption process through ion exchange with Cd^{2+}. More exchangeable ions and abundant functional groups served as the sorption/replacement sites for Cd, which attributed to good dispersion of the MF particles on the biochar matrix, were responsible for the elevated adsorption ability of

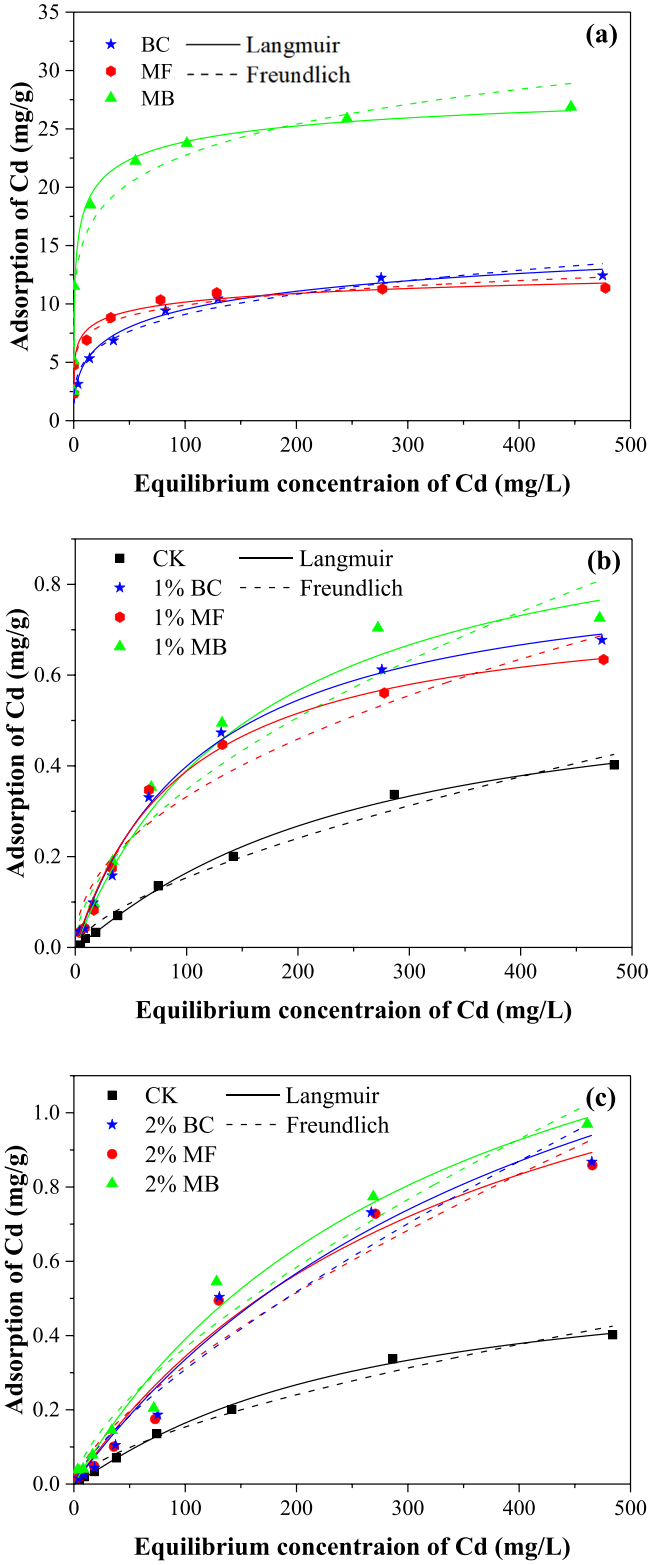

Fig. 3. Cadmium adsorption isotherms fitted with Langmuir and Freundlich models for BC, MF and MB in aqueous condition (a); amended-soils with 1% application rate (b) and 2% application rate (c). (cadmium concentration range: 5–500 mg/L, solution pH = 5.0, sorbent dosage for materials alone: 2 g/L, shaking speed = 180 rpm, equilibrium time = 24 h, temperature = 25 °C, n = 3).

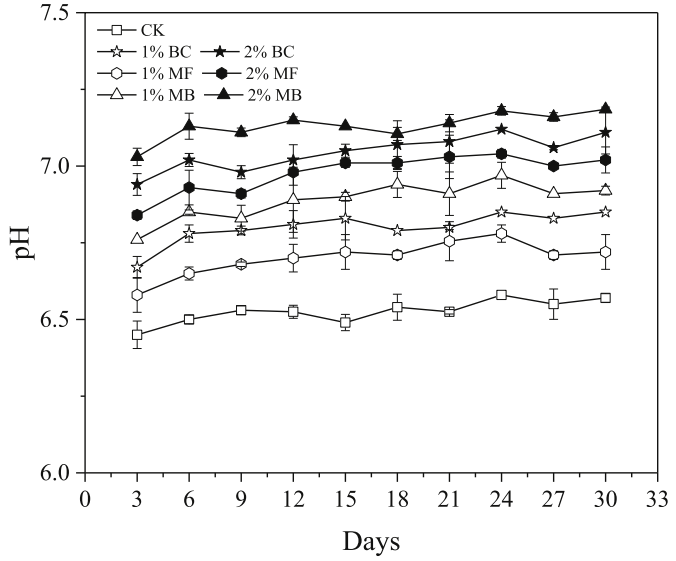

Fig. 4. The pH of the leachate in the different treatments over 30 days. (a total of 10 leaching events with three days intervals were performed. Treatments: CK: soil without amendment, 1% BC: soil amended with 1% BC, 1% MF: soil amended with 1% MF, 1% MB: soil amended with 1% MB, 2% BC: soil amended with 2% BC, 2% MF: soil amended with 2% MF, 2% MB: soil amended with 2% MB).

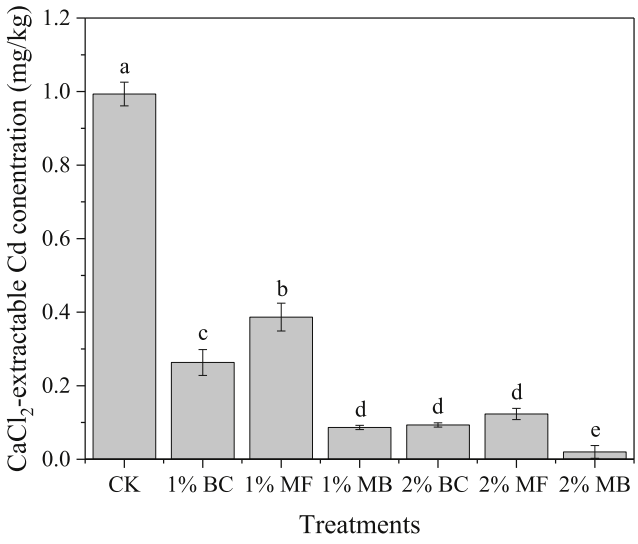

Fig. 5. The $CaCl_2$–Cd content of different treatments after 30 days incubation (different letters indicate significant differences among treatments at the $P < 0.05$ level.).

MB. Along with the significant increasement of pH, and consequently the higher passivation efficiency was obtained with MB-amended soil.

3.7. Early stage seeding growth bioassay

Previous researchers reported the effect of cadmium-induced stress on seeds germination as well as early-stage plant growth (Bai et al., 2014). However, the result of germination rate showed no variation among all treatments included soil without amendments (data not given here), implying no visible inhibition effect for pakchoi germination in the tested soil. Nevertheless, the root length increased dramatically after amendments by 1.22–3.98 folds ($P < 0.05$) (Fig. 6, Fig. S6), whereas the changes in shoot length were not significantly different for all treatments. Given the primary side effects of Cd on seed roots suggested previously (Lin et al., 2012; Lux et al., 2011), the results

Table 1
Isotherm parameters for cadmium adsorption by BC, MF, and MB and its amended soil fitted with Langmuir and Freundlich models.

Adsorbents/ Treatments	Medium	Langmuir			Freundlich		
		Q_{max} (mg/g)	*b* (L/mg)	R^2	K_f	1/n	R^2
BC	Aqueous	20.9	0.116	0.983	2.87	0.250	0.970
MF	Aqueous	17.3	0.428	0.968	5.21	0.139	0.950
MB	Aqueous	31.3	0.589	0.986	10.9	0.160	0.951
CK	Soil	0.594	0.00244	0.997	0.0079	0.645	0.983
1% BC	Soil	0.858	0.00376	0.995	0.0148	0.619	0.951
1% MF	Soil	0.768	0.00321	0.992	0.0129	0.639	0.942
1% MB	Soil	1.03	0.00396	0.989	0.0185	0.597	0.952
2% BC	Soil	1.71	0.00802	0.983	0.0364	0.489	0.968
2% MF	Soil	1.59	0.00606	0.975	0.0280	0.544	0.952
2% MB	Soil	1.85	0.00869	0.989	0.0385	0.468	0.949

Adsorbents: BC (biochar), MF (magnesium ferrite) and MB (magnesium ferrite biochar).
Treatments: CK: soil without amendment, 1% BC: soil amended with 1% biochar, 1% MF: soil amended with 1% magnesium ferrite, 1% MB: soil amended with 1% magnesium ferrite biochar, 2% BC: soil amended with 2% biochar, 2% MF: soil amended with 2% magnesium ferrite, 2% MB: magnesium ferrite biochar.

Table 2
The pH and EC under different treatments in soil after 30 days incubation.

Treatments	pH[a]	EC[a] (μS/cm)
CK	5.62 ± 0.01 g	272 ± 2.00 d
BC 1%	6.19 ± 0.02 d	197 ± 2.52 f
MF 1%	5.88 ± 0.03 f	288 ± 1.53 c
MB 1%	6.63 ± 0.03 b	209 ± 2.31 e
BC 2%	6.51 ± 0.02 c	209 ± 1.73 e
MF 2%	5.94 ± 0.01 e	362 ± 2.08 a
MB 2%	6.75 ± 0.04 a	318 ± 2.31 b

Data is expressed as mean ± SD (n = 3). Means followed by the same letters within the same column are not significantly different.
[a] pH and EC were measured using a 1:2.5 soil: water ratio.

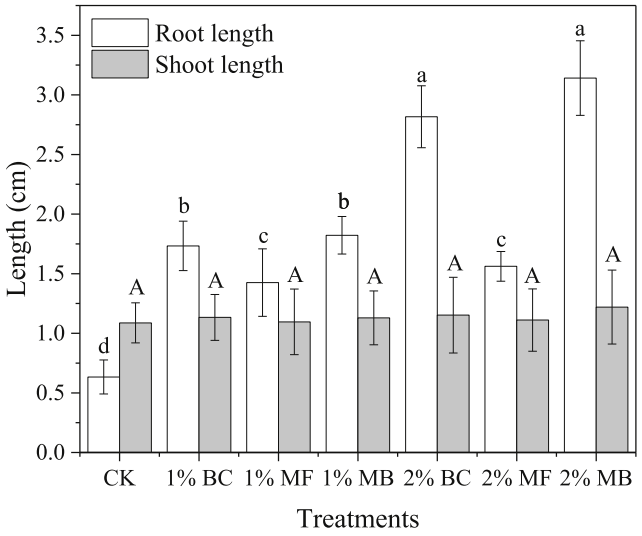

Fig. 6. Root and shoot length of packoi seeds as affected by different treatments from the natural Cd-polluted soil. (the error bars represent the standard deviation of the mean and same letters above the bar indicate that the results are not significantly different).

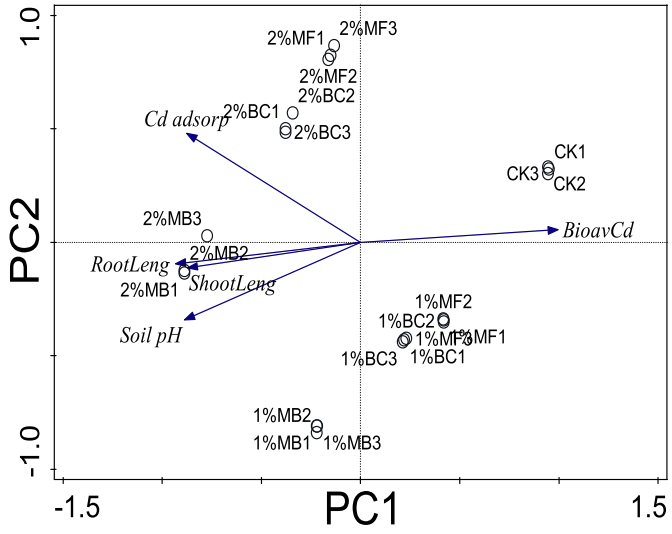

Fig. 7. Principle component analysis based on the soil/seeding parameters of different treatments. (parameters: soil pH: pH of amended soil; Cd adsorp: Cd adsorption capacity of amended soil; Bioav Cd: bioavailable-Cd content of amended soil; Root Leng: length of roots; and Shoot Leng: length of shoots.)

further supported the effective passivation of bioavailable Cd.

3.8. Multivariate statistical analysis

The principle component analysis was carried out to investigate the relationship among the various parameters as affected by the treatments (Fig. 7). The results revealed the soil pH had more strong relation with bioavailable Cd than adsorption capacity of amended soil. The length of roots and shoots showed a very close correlation by clearly clustering in the other spot opposite to bioavailable Cd. Basically, the soil pH and Cd adsorption capacity of amended soil govern the contents of bioavailable Cd. The mitigation of Cd-induced stress after incubation and the highest immobilization capacity of MB was confirmed since the 2% MB treatment and length of shoots/roots were clustered together.

4. Conclusions

The biochar, magnesium ferrite and magnesium ferrite biochar had been utilized to assess its immobilization effectiveness of Cd through sequential leaching, batch experiments, and early stage seeding bioassay experiments. The magnesium ferrite biochar presented the most promising adsorption/passivation ability than the pure biochar and ferrite. The elevated soil pH and adsorption capacity were ascribed to the synergistic effects between biochar and ferrite and hence it facilitated the Cd immobilization ability by magnesium ferrite biochar. In addition, Cd-induced stress in plant growth can be effectively alleviated by magnesium ferrite biochar application. Herein, the ferrite biochar composite could be used as a potential passivator for Cd-polluted soil. The suitability of the engineered biochars for different soils and contaminants will be tested to facilitate their future scale-up applications.

Acknowledgement

We gratefully acknowledge the financial support of China Agricultural Research Service (CARS-23-B16), the National Natural Science Foundation of China (Grant No. 51709103), Hong Kong Scholars Program (Grant No. XJ2018029).

Appendix A. Supplementary data

Supplementary data to this article can be found online at https://

doi.org/10.1016/j.jenvman.2019.109610.

References

Bai, J., Huang, L., Gao, Z., Lu, Q., Wang, J., Zhao, Q., 2014. Soil seed banks and their germination responses to cadmium and salinity stresses in coastal wetlands affected by reclamation and urbanization based on indoor and outdoor experiments. J. Hazard Mater. 280, 295–303.

Bashir, S., Adeel, M., Gulshan, A.B., Iqbal, J., Khan, S., Rehman, M., Azeem, M., 2019. Effects of organic and inorganic passivators on the immobilization of cadmium in contaminated soils: a review. Environ. Eng. Sci. 0 0, 0.

Beesley, L., Marmiroli, M., 2011. The immobilisation and retention of soluble arsenic, cadmium and zinc by biochar. Environ. Pollut. 159, 474–480.

Beiyuan, J., Awad, Y.M., Beckers, F., Tsang, D.C., Ok, Y.S., Rinklebe, J., 2017. Mobility and phytoavailability of as and Pb in a contaminated soil using pine sawdust biochar under systematic change of redox conditions. Chemosphere 178, 110–118.

Chen, H., Teng, Y., Lu, S., Wang, Y., Wang, J., 2015. Contamination features and health risk of soil heavy metals in China. Sci. Total Environ. 512–513, 143–153.

Chen, Z., Liu, T., Tang, J., Zheng, Z., Wang, H., Shao, Q., Chen, G., Li, Z., Chen, Y., Zhu, J., Feng, T., 2018. Characteristics and mechanisms of cadmium adsorption from aqueous solution using lotus seedpod-derived biochar at two pyrolytic temperatures. Environ. Sci. Pollut. Res. Int. 25, 11854–11866.

Cui, J., Jin, Q., Li, Y., Li, F., 2019a. Oxidation and removal of as (III) from soil using novel magnetic nanocomposite derived from biomass waste. Environ. Sci. Nano. 6, 478–488.

Cui, L., Noerpel, M.R., Scheckel, K.G., Ippolito, J.A., 2019b. Wheat straw biochar reduces environmental cadmium bioavailability. Environ. Int. 126, 69–75.

Eyvazi, B., Jamshidi-Zanjani, A., Khodadadi Darban, A., 2019. Immobilization of hexavalent chromium in contaminated soil using nano-magnetic $MnFe_2O_4$. J. Hazard Mater. 365, 813–819.

Fang, S., Tsang, D.C., Zhou, F., Zhang, W., Qiu, R., 2016. Stabilization of cationic and anionic metal species in contaminated soils using sludge-derived biochar. Chemosphere 149, 263–271.

Garrido-Rodriguez, B., Cutillas-Barreiro, L., Fernandez-Calvino, D., Arias-Estevez, M., Fernandez-Sanjurjo, M.J., Alvarez-Rodriguez, E., Nunez-Delgado, A., 2014. Competitive adsorption and transport of Cd, Cu, Ni and Zn in a mine soil amended with mussel shell. Chemosphere 107, 379–385.

Gong, Y., Zhao, D., Wang, Q., 2018. An overview of field-scale studies on remediation of soil contaminated with heavy metals and metalloids: technical progress over the last decade. Water Res. 147, 440–460.

Gwenzi, W., Chaukura, N., Noubactep, C., Mukome, F.N.D., 2017. Biochar-based water treatment systems as a potential low-cost and sustainable technology for clean water provision. J. Environ. Manag. 197, 732–749.

Houba, V.J.G., Temminghoff, E.J.M., Gaikhorst, G.A., van Vark, W., 2008. Soil analysis procedures using 0.01 M calcium chloride as extraction reagent. Commun. Soil. Sci. Plan. 31, 1299–1396.

Hudcova, B., Vitkova, M., Ourednicek, P., Komarek, M., 2019. Stability and stabilizing efficiency of Mg-Fe layered double hydroxides and mixed oxides in aqueous solutions and soils with elevated as (V), Pb (II) and Zn (II) contents. Sci. Total Environ. 648, 1511–1519.

Igalavithana, A.D., Park, J., Ryu, C., Lee, Y.H., Hashimoto, Y., Huang, L., Kwon, E.E., Ok, Y.S., Lee, S.S., 2017. Slow pyrolyzed biochars from crop residues for soil metal(loid) immobilization and microbial community abundance in contaminated agricultural soils. Chemosphere 177, 157–166.

Jung, K.W., Lee, S., Lee, Y.J., 2017. Synthesis of novel magnesium ferrite ($MgFe_2O_4$)/biochar magnetic composites and its adsorption behavior for phosphate in aqueous solutions. Bioresour. Technol. 245, 751–759.

Karunanayake, A.G., Todd, O.A., Crowley, M., Ricchetti, L., Pittman, C.U., Anderson, R., Mohan, D., Mlsna, T., 2018. Lead and cadmium remediation using magnetized and nonmagnetized biochar from Douglas fir. Chem. Eng. J. 331, 480–491.

Khan, M.A., Khan, S., Ding, X., Khan, A., Alam, M., 2018. The effects of biochar and rice husk on adsorption and desorption of cadmium on to soils with different water conditions (upland and saturated). Chemosphere 193, 1120–1126.

Li, Y.J., Li, L., Wang, G.L., Song, S., Sun, Y.Y., 2016. In-situ remediation of lead–zinc polymetallic mine contaminated soils by $MnFe_2O_4$ microparticles. Soil Sediment Contam. 25, 356–364.

Li, N., Yin, M., Tsang, D., Yang, S., Liu, J., Li, X., Song, G., Wang, J., 2019. Mechanisms of U(VI) removal by biochar derived from Ficus microcarpa aerial root: a comparison between raw and modified biochar. Sci. Total Environ. 697 (134115).

Lin, J., Su, B., Sun, M., Chen, B., Chen, Z., 2018. Biosynthesized iron oxide nanoparticles used for optimized removal of cadmium with response surface methodology. Sci. Total Environ. 627, 314–321.

Lin, L., Zhou, W., Dai, H., Cao, F., Zhang, G., Wu, F., 2012. Selenium reduces cadmium uptake and mitigates cadmium toxicity in rice. J. Hazard Mater. 235–236, 343–351.

Liu, J., Li, N., Zhang, W., Wei, X., Tsang, D., Sun, Y., Luo, X., Bao, Z., Zheng, W., Wang, J., Xu, G., Hou, L., Chen, Y., Feng, Y., 2019. Thallium contamination in farmlands and common vegetables in a pyrite mining city and potential health risks. Environ. Pollut. 248, 906–915.

Liu, J., Yin, M., Zhang, W., Tsang, D., Wei, X., Zhou, Y., Xiao, T., Wang, J., Dong, X., Sun, Y., Chen, Y., Li, H., Hou, L., 2019. Response of microbial communities and interactions to thallium in contaminated sediments near a pyrite mining area. Envrion. Pollut. 248, 916–928.

Liu, J., Ren, S., Zhou, Y., Tsang, D., Lippold, H., Wang, J., Yin, M., Xiao, T., Luo, X., Chen, Y., 2019. High contamination risks of thallium and associated metal(loid)s in fluvial sediments from a steel-making area and implications for environmental management. J. Environ. Manage. 250 (109513).

Liu, J., Luo, X., Sun, Y., Tsang, D., Qi, J., Zhang, W., Yin, M., Wang, J., Lippold, H., Chen, Y., Sheng, G., 2019. Thallium pollution in China and removal technologies for waters: a review. Environ. Int. 126, 771–790 In preparation.

Liu, T., Li, F., Jin, Z., Yang, Y., 2018. Acidic leaching of potentially toxic metals cadmium, cobalt, chromium, copper, nickel, lead, and zinc from two Zn smelting slag materials incubated in an acidic soil. Environ. Pollut. 238, 359–368.

Loganathan, P., Vigneswaran, S., Kandasamy, J., Naidu, R., 2012. Cadmium sorption and desorption in soils: a review. Crit. Rev. Environ. Sci. Technol. 42, 489–533.

Lu, H.P., Li, Z.A., Gasco, G., Mendez, A., Shen, Y., Paz-Ferreiro, J., 2018. Use of magnetic biochars for the immobilization of heavy metals in a multi-contaminated soil. Sci. Total Environ. 622–623, 892–899.

Lu, K., Yang, X., Gielen, G., Bolan, N., Ok, Y.S., Niazi, N.K., Xu, S., Yuan, G., Chen, X., Zhang, X., Liu, D., Song, Z., Liu, X., Wang, H., 2017. Effect of bamboo and rice straw biochars on the mobility and redistribution of heavy metals (Cd, Cu, Pb and Zn) in contaminated soil. J. Environ. Manag. 186, 285–292.

Lux, A., Martinka, M., Vaculik, M., White, P.J., 2011. Root responses to cadmium in the rhizosphere: a review. J. Exp. Bot. 62, 21–37.

Mahato, D.K., Majumder, S., Banerjee, S., 2017. Large polaron tunneling, magnetic and impedance analysis of magnesium ferrite nanocrystallite. Appl. Surf. Sci. 413, 149–159.

Mittal, V.K., Bera, S., Nithya, R., Srinivasan, M.P., Velmurugan, S., Narasimhan, S.V., 2004. Solid state synthesis of Mg–Ni ferrite and characterization by XRD and XPS. J. Nucl. Mater. 335, 302–310.

Ouředníček, P., Hudcová, B., Trakal, L., Pohořelý, M., Komárek, M., 2019. Synthesis of modified amorphous manganese oxide using low-cost sugars and biochars: material characterization and metal(loid) sorption properties. Sci. Total Environ. 670, 1159–1169.

Pardo, J., Mondaca, P., Celis-Diez, J.L., Ginocchio, R., Navarro-Villarroel, C., Neaman, A., 2018. Assessment of revegetation of an acidic metal(loid)-polluted soils six years after the incorporation of lime with and without compost. Geoderma 331, 81–86.

Peng, D., Wu, B., Tan, H., Hou, S., Liu, M., Tang, H., Yu, J., Xu, H., 2019a. Effect of multiple iron-based nanoparticles on availability of lead and iron, and micro-ecology in lead contaminated soil. Chemosphere 228, 44–53.

Peng, Y., Sun, Y., Sun, R., Zhou, Y., Tsang, D.C.W., Chen, Q., 2019b. Optimizing the synthesis of Fe/Al (Hydr)oxides-Biochars to maximize phosphate removal via response surface model. J. Clean. Prod. 237, 117770.

Puga, A.P., Melo, L.C.A., de Abreu, C.A., Coscione, A.R., Paz-Ferreiro, J., 2016. Leaching and fractionation of heavy metals in mining soils amended with biochar. Soil. Till. Res. 164, 25–33.

Qiao, J.T., Liu, T.X., Wang, X.Q., Li, F.B., Lv, Y.H., Cui, J.H., Zeng, X.D., Yuan, Y.Z., Liu, C.P., 2018. Simultaneous alleviation of cadmium and arsenic accumulation in rice by applying zero-valent iron and biochar to contaminated paddy soils. Chemosphere 195, 260–271.

Qin, P., Wang, H., Yang, X., He, L., Muller, K., Shaheen, S.M., Xu, S., Rinklebe, J., Tsang, D.C.W., Ok, Y.S., Bolan, N., Song, Z., Che, L., Xu, X., 2018. Bamboo- and pig-derived biochars reduce leaching losses of dibutyl phthalate, cadmium, and lead from co-contaminated soils. Chemosphere 198, 450–459.

Rehman, M.Z.U., Rizwan, M., Khalid, H., Ali, S., Naeem, A., Yousaf, B., Liu, G., Sabir, M., Farooq, M., 2018. Farmyard manure alone and combined with immobilizing amendments reduced cadmium accumulation in wheat and rice grains grown in field irrigated with raw effluents. Chemosphere 199, 468–476.

Shi, Z., Allen, H.E., Di Toro, D.M., Lee, S.Z., Flores Meza, D.M., Lofts, S., 2007. Predicting cadmium adsorption on soils using WHAM VI. Chemosphere 69, 605–612.

Trakal, L., Veselska, V., Safarik, I., Vitkova, M., Cihalova, S., Komarek, M., 2016. Lead and cadmium sorption mechanisms on magnetically modified biochars. Bioresour. Technol. 203, 318–324.

Wan, Z., Sun, Y., Tsang, D.C.W., Yu, I.K.M., Fan, J., Clark, J.H., Zhou, Y., Cao, X., Gao, B., Ok, Y.S., 2019. A sustainable biochar catalyst synergized with copper heteroatoms and CO_2 for singlet oxygenation and electron transfer routes. Green Chem. 21, 4800–4814.

Wang, B., Gao, B., Fang, J., 2018a. Recent advances in engineered biochar productions and applications. Crit. Rev. Environ. Sci. Technol. 47, 2158–2207.

Wang, G., Zhang, S., Zhong, Q., Xu, X., Li, T., Jia, Y., Zhang, Y., Peijnenburg, W., Vijver, M.G., 2018b. Effect of soil washing with biodegradable chelators on the toxicity of residual metals and soil biological properties. Sci. Total Environ. 625, 1021–1029.

Wang, Y., Ji, H., Lyu, H., Liu, Y., He, L., You, L., Zhou, C., Yang, S., 2019. Simultaneous alleviation of Sb and Cd availability in contaminated soil and accumulation in Lolium multiflorum Lam. After amendment with Fe–Mn-Modified biochar. J. Clean. Prod. 231, 556–564.

Wu, C., Shi, L., Xue, S., Li, W., Jiang, X., Rajendran, M., Qian, Z., 2019. Effect of sulfur-iron modified biochar on the available cadmium and bacterial community structure in contaminated soils. Sci. Total Environ. 647, 1158–1168.

Xia, R., Peng, Y., Zhong, S., Tu, L., Xie, Y., Zhang, L., 2017. Performance of the iron-caron coupling constructed wetland for rural sewage treatment. IOP Conf. Ser. Earth Environ. Sci. 012–016.

Xiang, Y., Xu, Z., Wei, Y., Zhou, Y., Yang, X., Yang, Y., Yang, J., Zhang, J., Luo, L., Zhou, Z., 2019a. Carbon-based materials as adsorbent for antibiotics removal: mechanisms and influencing factors. J. Environ. Manag. 237, 128–138.

Xiang, Y., Xu, Z., Zhou, Y., Wei, Y., Long, X., He, Y., Zhi, D., Yang, J., Luo, L., 2019b. A sustainable ferromanganese biochar adsorbent for effective levofloxacin removal from aqueous medium. Chemosphere 237, 124464.

Xiong, W., Zeng, Z., Zeng, G., Yang, Z., Xiao, R., Li, X., Cao, J., Zhou, C., Chen, H., Jia, M., Yang, Y., Wang, W., Tang, X., 2019. Metal-organic frameworks derived magnetic carbon-αFe/Fe_3C composites as a highly effective adsorbent for tetracycline removal from aqueous solution. Chem. Eng. J. 374, 91–99.

Xu, Y., Liang, X., Xu, Y., Qin, X., Huang, Q., Wang, L., Sun, Y., 2017. Remediation of heavy metal-polluted agricultural soils using clay minerals: a review. Pedosphere 27, 193–204.

Yang, F., Zhang, S., Sun, Y., Tsang, D.C.W., Cheng, K., Ok, Y.S., 2019. Assembling biochar with various layered double hydroxides for enhancement of phosphorus recovery. J. Hazard Mater. 365, 665–673.

Yang, X., Igalavithana, A.D., Oh, S.E., Nam, H., Zhang, M., Wang, C.H., Kwon, E.E., Tsang, D.C.W., Ok, Y.S., 2018. Characterization of bioenergy biochar and its utilization for metal/metalloid immobilization in contaminated soil. Sci. Total Environ. 640–641, 704–713.

Yin, M., Sun, J., Chen, Y., Wang, J., Shang, J., Belshaw, N., Shen, C., Liu, J., Li, H., Linghu, W., Xiao, T., Dong, X., Song, G., Xiao, E., Chen, D., 2019. Mechanism of uranium release from uranium mill tailings under long-term exposure to simulated acid rain: geochemical evidence and environmental implication. Environ. Pollut.

Yin, Z., Liu, Y., Liu, S., Jiang, L., Tan, X., Zeng, G., Li, M., Liu, S., Tian, S., Fang, Y., 2018. Activated magnetic biochar by one-step synthesis: enhanced adsorption and coadsorption for 17 beta-estradiol and copper. Sci. Total Environ. 639, 1530–1542.

Yin, D., Wang, X., Chen, C., Peng, B., Tan, C., Li, H., 2016. Varying effect of biochar on Cd, Pb and as mobility in a multi-metal contaminated paddy soil. Chemosphere 152, 196–206.

Yoo, J.C., Beiyuan, J., Wang, L., Tsang, D.C.W., Baek, K., Bolan, N.S., Ok, Y.S., Li, X.D., 2018. A combination of ferric nitrate/EDDS-enhanced washing and sludge-derived biochar stabilization of metal-contaminated soils. Sci. Total Environ. 616–617, 572–582.